JOURNAL OF SOLID STATE CHEMISTRY **122,** 31–35 (1996)
ARTICLE NO. 0077

Synthesis, Crystal Structure, and Electronic Structure of $CsCuFeS_2$

Jaime Llanos,* Patricio Valenzuela, Carlos Mujica, and Antonio Buljan

Departamento de Química, Facultad de Ciencias, Universidad Católica del Norte, Casilla 1280, Antofagasta, Chile

and

Rafael Ramírez

Instituto de Ciencia de Materiales, CSIC, Serrano 115 dpdo., 28006 Madrid, Spain

Received July 12, 1995; in revised form October 30, 1995; accepted November 2, 1995

The new chalcogenide $CsCuFeS_2$ has been prepared by solid state reaction of stoichiometric amounts of $CuFeS_2$ and Cs_2CO_3 at 1280 K. This phase crystallizes in the $ThCr_2Si_2$-type structure with space group $I4/mmm$ (No. 139), $Z = 2$, and cell constants $a = 394.2(1)$ pm, and $c = 1423.8(9)$ pm. The discrepancy indices of the single-crystal structure refinement were $R = 0.054$ and $R_w = 0.050$. The sulfur atoms form layers of edge-sharing square pyramids pointing up and down with their apices. The Cu and Fe atoms are located in the remaining tetrahedral holes, while the Cs atoms are found in the interlayer region coordinated to eight sulfur atoms, forming a cube elongated along the c axis. The electronic structure is analyzed by means of extended Hückel tight-binding calculations. Our results show that this compound should be a metal and that the interactions between the transition metals atoms are largest for Fe–Fe pairs. © 1996 Academic Press, Inc.

INTRODUCTION

A series of new compounds made of alkali metals, copper, iron, and sulfur or selenium atoms, which are based on a common structural pattern consisting of two-dimensional (2D) arrangements of chalcogen tetrahedra linked by edges, has been recently synthesized. The centers of the tetrahedra are occupied by the transition metal atoms (Cu,Fe) in a ratio 1 : 1. The crystal structures of the phases $MCuFeX_2$ (M = Li, Na or K; X = S or Se) have been recently reported (1–3) and the electronic structure and distribution of (Cu,Fe) atoms in $LiCuFeS_2$ and $NaCuFeS_2$ have been studied by extended Hückel (EH) calculations (4) and Monte Carlo simulations (5). The crystallographic data derived from single-crystal investigations of these compounds showed partial differences with other transition metals dichalcogenides. The alkali metals in the layered compounds $MTiS_2$ or $MZrS_2$, with M = Li, Na, K, and Cs, always have coordination number of six, with octahedral, trigonal prismatic, or trigonal antiprismatic symmetry (6). Similarly, the Li or Na atoms intercalated in chalcopyrite, $CuFeS_2$, or eskeborite, $CuFeS_2$, occupy the sites with octahedral symmetry. However, the intercalation of K results in a occupation of sites with cubic coordination.

We have found a new member of the $MCuFeX_2$ family, with M = Cs, whose synthesis, crystal structure, and electronic structure are described in this article.

EXPERIMENTAL

Synthesis. $CuFeS_2$ and Cs_2CO_3 constitute the starting materials for the compound preparation. Synthetic chalcopyrite was prepared as described in literature (7). The X-ray powder diffraction diagram of $CuFeS_2$ did not show any extraneous lines. Cs_2CO_3 was nominally 99.5% pure (Sigma) and no impurities were detected on examination of its X-ray powder diagram. Stoichiometric amounts of $CuFeS_2$ and Cs_2CO_3 were mixed in a sealed graphite crucible and heated at 1280 K for 48 hours. At the end of the reaction, the sample was cooled down slowly to room temperature by cutting off the power of the furnace.

The powder diffraction diagram of the product of the reaction was examined for peaks from the starting materials, from binary or ternary (Cu,Fe) sulfides, and from possible isostructural compounds, such as $KCuFeS_2$. First inspection of the powder patterns did not reveal a close relationship between $KCuFeS_2$ and $CsCuFeS_2$, because the intensity of the ($00l$) reflections are different. However, subsequents refinements of the structural data of $CsCuFeS_2$ showed that both phases are isostructural.

Crystallography. A single crystal of the well-crystallized $CsCuFeS_2$ compound was selected and mounted into a glass capillary for the X-ray analysis with a four-circle diffractometer (Siemens R3m/V) using graphite mono-

* To whom correspondence should be addressed.

0022-4596/96 $18.00

TABLE 1
Crystallographic Data and Details of the Structure Analysis for $CsCuFeS_2$

Formula	$CsCuFeS_2$
Crystal system	Tetragonal
Space group	*I*4/*mmm* (No. 139)
a (pm)	394.2(1)
c (pm)	1423.8(9)
Z	2
Volume (10^6 pm^3)	221.25(6)
μ Mo$K\alpha$ (cm^{-1})	161.93
Diffractometer	Siemens R3m/V
Radiation, monochromator	Mo$K\alpha$, Graphite
Scanning mode	ω-2θ
2θ max.	45
Measured reflections	450
Unique reflections	149
Number of refined parameters	9
Final R,[a] R_w[b]	0.054, 0.050

[a] $R = \Sigma(|F_o| - |F_c|)/\Sigma|F_o|$.
[b] $R_w = \{\Sigma[w(|F_o| - |F_c|)^2]/\Sigma(wF_o^2)\}^{1/2}$; $w = 2.7[\sigma^2(F)]$.

chromated Mo$K\alpha$ radiation. Cell parameters were refined from 20 centered reflections. Intensities were measured in the ω-2θ scan mode and the absorption correction was done empirically by ψ scanning.

The structure refinement was made with the program system SHELX-76 (8) starting with the atomic positions of Th, Cr, and Si of $ThCr_2Si_2$ (9) as initial guess for the Cs, (Cu,Fe), and S coordinates, respectively. Bond distances and angles were calculated using the program ORFFE (10). The crystallographic data as well as details of the structure analysis of $CsCuFeS_2$ are given in Table 1.

CRYSTAL STRUCTURE OF $CsCuFeS_2$

The refined atomic coordinates, anisotropic displacement parameters, and site occupation factors of $CsCuFeS_2$ are listed in Table 2. The S.O.F. of copper and iron in position 4d was fixed at a value of 0.5. Some relevant interatomic distances and bond angles are given in Table 3.

The new synthetized cesium, copper, and iron sulfide adopts the $ThCr_2Si_2$-type structure and is isostructural with the already reported chalcogenides $KCuFeS_2$, $BaCu_2S_2$, and $TlCu_2S_2$ (3, 11). Its crystal structure can be described as a 2D arrangement of square pyramids of sulfur atoms pointing up and down with their apices. They are connected by sharing all edges. Copper and iron atoms are distributed in the ratio 1:1 in the remaining tetrahedral holes. The alkali metal ions are located between two different layers. This arrangement provides a tetrahedral coordination for the transition metals atoms and an eightfold coordination for the cesium ions. A perspective view of $CsCuFeS_2$ is shown in Fig. 1.

In $KCuFeS_2$, the tetrahedra formed by the S atoms, whose centers are occupied by the transition metals atoms, are regular. However, in $CsCuFeS_2$ the tetrahedra are slight distorted and we find two different S–Fe–S angles around the transition metal (108.3° and 111.9°). The cubes formed by the eight S atoms closest to the Cs position are almost regular, with Cs–S distances of 356.8 pm. The angles at the sulfur corners amount to 90°. Nevertheless, the angles around the Cs^+ ion reveal a tetragonal distortion of the cube, where the eight S–S edges belonging to the

TABLE 2
Fractional Atomic Coordinates, and Equivalent and Anisotropic Displacement Parameters (in pm^2, $U_{11} = U_{22}$; $U_{12} = U_{13} = U_{23} = 0$)

Atom	Position	*x*	*y*	*z*	S.O.F.	U_{eq}	U_{11}	U_{33}
Cs	2a	0	0	0	1	254(5)	218(7)	328(11)
Cu	4d	0	½	¼	0.5	201(6)	121(7)	316(16)
Fe	4d	0	½	¼	0.5	201(6)	121(7)	316(16)
S	4e	0	0	0.3436(3)	1	196(9)	134(11)	321(22)

Note. Standard deviations are given in parentheses.

TABLE 3
Selected Interatomic Distances (pm) and Angles (°) with Standard Deviation Given in Parentheses

Interatomic distances		Bond angles	
M–S	237.9(3) × 4	S–*M*–S	108.3(1) × 4
M–*M*	278.7(5) × 4	S–*M*–S	111.9(2) × 2
S–S (intralayer, diff. *z*)	385.6(7)	S–Cs–S	67.06(7) × 8
S–S (intralayer, equal *z*)	394.2(1) × 4	S–Cs–S	112.94(7) × 8
S–S (interlayer)	445.0(1)	S–Cs–S	102.7(1) × 4
Cs–S	356.8(3) × 8	S–Cs–S	77.3(1) × 4

Note. *M* = Cu, Fe.

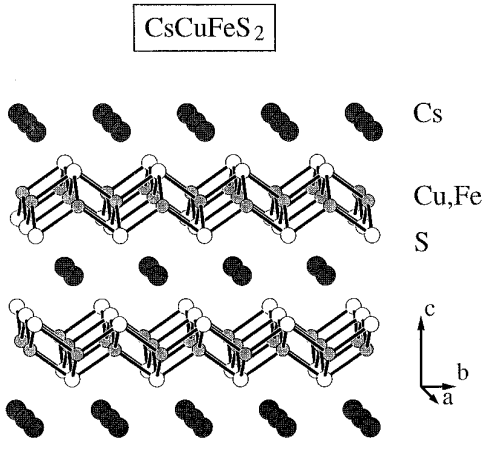

FIG. 1. Crystal structure of $CsCuFeS_2$.

TABLE 4
Extended Hückel Parameters

Atom	Orbital	H_{ii} (eV)	ξ_1	ξ_2	c_1	c_2
S	3s	−20.00	2.122			
	3p	−13.30	1.827			
Cu	4s	−11.40	2.200			
	4p	−6.06	2.200			
	3d	−14.00	5.950	2.30	0.5933	0.5744
Fe	4s	−9.10	1.900			
	4p	−5.32	1.900			
	3d	−12.60	5.350	2.00	0.5505	0.6260

Note. H_{ii} are diagonal matrix elements of the EH Hamiltonian, ξ_i are the Slater exponents, and c_i are the expansion coefficients.

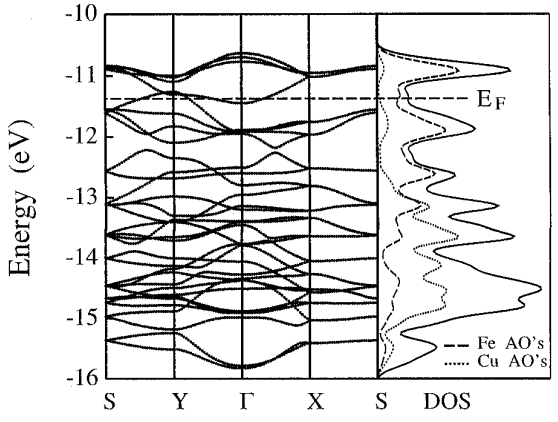

FIG. 2. EH band structure diagram for a single $[CuFeS_2]^{-1}$ layer. The total DOS curve (continuous line) as well as the projected DOS curves for the Fe AOs (broken line) and Cu AOs (dotted line) are displayed. The Fermi level is indicated by the label E_F.

same layer are smaller (394.2 pm) than the four S–S edges with sulfur atoms belonging to different layers (445.0 pm).

ELECTRONIC STRUCTURE OF $CsCuFeS_2$

EH tight-binding calculations (12–15) for investigating the band structure of $CsCuFeS_2$ were performed. The transfer of the valence electrons from the alkali metal atoms toward the $CuFeS_2$ layer is almost complete. Therefore, we have adopted the 2D model $[CuFeS_2]^{-1}$ for our electronic structure calculations. We have chosen for the band structure calculations a 2D square supercell with lattice parameter $a\sqrt{2}$ with the (Cu,Fe) atoms distributed in the tetrahedral sites with an ordering pattern that maximizes the number of Fe–Fe pairs. The extended Hückel parameters used in the calculations are given in Table 4. These values were taken from the literature (16–18). The off-diagonal matrix elements of the Hamiltonian were evaluated by means of a weighted formula (19). A set of 120 k points in the irreducible part of the Brillouin zone was used for the density of state (DOS) calculations (20, 21).

Analysis of the orbital character of the bands reveals that in the energy region between −10 and −16 eV there appear admixtures of S 3*p*, Fe 3*d*, and Cu 3*d* orbitals. The S 3*s* bands are found at lower energies (around −22 eV) and are not shown in the figure. The energy bands and DOS curve of a $[CuFeS_2]^{-1}$ layer are displayed in Fig. 2. The projected DOS distributions for Fe and Cu atomic orbitals (AOs) are also given in the figure. The Fermi energy crosses the valence band, and, therefore, metallic conductivity within the 2D layers is expected for $CsCuFeS_2$.

The energy bands at the Fermi level have mainly Fe 3*d* character. The maximum in the DOS curve associated with the Cu 3*d* orbitals is found about 3 eV below the Fermi level.

In the layer $[CuFeS_2]^{-1}$, the shortest Fe–S or Cu–S distance is 237.9 pm and the shortest Cu–Cu, Cu–Fe, or Fe–Fe distance is 278.7 pm. The latter is definitely in the metal–metal bonding range (22). The crystal orbital overlap population (COOP) curves in Fig. 3 indicate that the Cu–S and the Fe–S interactions at the bottom of the displayed energy region are strongly bonding, whereas the electronic states around the Fermi level are Cu–S antibonding and slightly Fe–S bonding. The metal–metal COOP curves in Fig. 4 show that the metal–metal contacts are mainly bonding except near the Fermi level, where they are antibonding. The largest bonding Fe–Fe interactions are found slightly above −13 eV, whereas the Cu–Cu and Cu–Fe are comparatively weak.

The integration of the COOP curves up to the Fermi level results in the overlap population indices shown in Table 5. The small positive Cu–Cu overlap population is

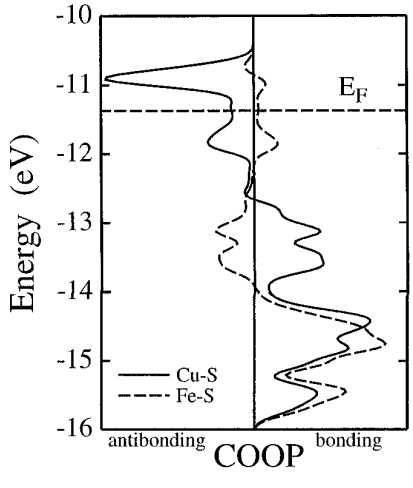

FIG. 3. COOP curves of Cu–S and Fe–S bonds. The position of the Fermi level is shown by a horizontal line.

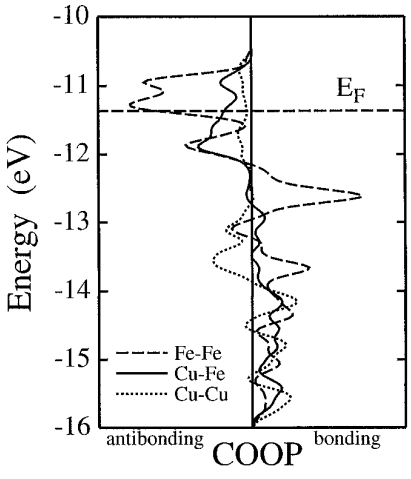

FIG. 4. COOP curves of Fe–Fe, Cu–Cu, and Cu–Fe pairs in $[CuFeS_2]^{-1}$. The position of the Fermi level is shown by a horizontal line. The curves are displayed in the same scale as those in Fig. 3.

comparable to that reported in the $BaCu_2S_2$ (0.021) phase and can be attributed to second-order mixing of Cu 4*s* and 4*p* states into occupied levels (11). The largest metal–metal interactions correspond to Fe–Fe pairs in agreement with the results of EH calculations for $NaCuFeS_2$ (5).

An outstanding chemical property of $CsCuFeS_2$ is the reaction with water and other protonic solvents, leading to the topotactic formation of a new metastable $CuFeS_2$ modification according to

$$CsCuFeS_2\,(s) + H_2O(l) \rightarrow CuFeS_2 + \tfrac{1}{2}H_2\,(g) + Cs^+(aq) + OH^-(aq).$$

The removal of Cs^+ cations and the subsequent oxidation of the layer structure to $CuFeS_2$ enhances the metal–metal and metal–sulfur interactions in the $CuFeS_2$ layer, because the top of the valence band has antibonding character for Cu–Cu, Cu–Fe, Fe–Fe, and Cu–S pairs. This fact leads us to assume the possibility of intercalating into the van der Waals gap of this new metastable $CuFeS_2$-modification species like amines or other Lewis bases.

TABLE 5
Overlap Population Indices of Selected Bonds in a $[CuFeS_2]^{-1}$ Layer

Bond	Index
Cu–Cu	0.034
Cu–Fe	0.055
Fe–Fe	0.141
Fe–S	0.384
Cu–S	0.285

CONCLUSIONS

$CsCuFeS_2$ crystallizes in the $ThCr_2Si_2$-type structure and is one of the few examples of chalcogenides of d^{10} transition metals found with this structure. EH tight-binding calculations show that this compound is a metal and that the interactions between the transition metal atoms are largest for the Fe–Fe pairs. This result might be relevant for the magnetic properties of this compound. We have not tried to study electronic configurations with spin polarization as the electron–electron interactions are completely neglected in the EH Hamiltonian.

On the other hand, the removal of Cs^+ is possible without destroying the 2D structure of the $CuFeS_2$ layer. In this way, a new material with the composition of chalcopyrite is obtained that is expected to act as the host compound in intercalation reactions. Further work in hopes of intercalating poliethylenoxide (PEO) into this metastable $CuFeS_2$ phase is in progress.

ACKNOWLEDGMENTS

This work was supported by Fondecyt Contracts 92/586 and 1941129, and by the Programa de Intercambio Académico Fundación Andes-Conicyt (Chile)–CSIC (Spain). The authors thank Professor O. Wittke for measurements on a Siemens diffractometer that was financed by Fundación Andes C/10810.

REFERENCES

1. J. Llanos, C. Contreras, C. Mujica, H. G. von Schnering, and K. Peters, *Mater. Res. Bull.* **28,** 39 (1993).
2. J. Llanos, J. Páez, C. Contreras, M. Guzmán, and C. Mujica, *J. Alloys Compd.* **201,** 103 (1994).
3. C. Mujica, J. Páez and J. Llanos, *Mater. Res. Bull.* **29,** 263 (1994).
4. J. Llanos, A. Buljan, C. Mujica, and R. Ramírez, *Mater. Res. Bull.* **30,** 43 (1995).
5. R. Ramírez, A. Buljan, J. C. Noya, and J. Llanos, *Chem. Phys.* **189,** 585 (1994).
6. M. S. Whittingham, *Prog. Solid State Chem.* **12,** 41 (1978).
7. D. B. Roberts and D. J. Williams, *Mater. Res. Bull.* **10,** 163 (1975).
8. G. Sheldrix, "SHELX Program for Crystal Structure Determination, Version 76." Cambridge Univ. Press, Cambridge, 1976.
9. Z. Ban and M. Zikirica, *Acta Crystallogr.* **18,** 594 (1965).
10. W. R. Bunsing, K. O. Martin, and H. A. Levy, ORFFE, Rapport, ORNL-TM-306. Oak Ridge Laboratory, Tennessee 1964
11. A. Ouammou, M. Mouallem-Bahout, O. Peña, J. F. Halet, J-Y. Saillard, and C. Carel, *J. Solid State Chem.* **117,** 73 (1995).
12. N. Y. Ashcroft and N. D. Mermin, "Solid State Physics." Holt, Rinehart and Winston, New York, 1976.
13. M.-H. Whangbo and R. Hoffmann, *J. Am. Chem. Soc.* **100,** 6093 (1978).
14. M.-H. Whangbo, R. Hoffmann, and R. B. Woodward, *Proc. R. Soc. London Ser. A* **366,** 23 (1979).

15. R. Hoffmann and W. N. Lipscomb, *J. Chem. Phys.* **36,** 2176 (1962); R. Hoffmann, *J. Chem. Phys.* **39,** 1397 (1963).
16. P. J. Hay, J. C. Thibeault, and R. Hoffmann, *J. Am. Chem. Soc.* **97,** 4884 (1975).
17. R. H. Summerville and R. Hoffmann, *J. Am. Chem. Soc.* **98,** 7240 (1976).
18. M. M. L. Chen and R. Hoffmann, *J. Am. Chem. Soc.* **98,** 1647 (1976).
19. J. H. Ammeter, H-B. Bürgi, J. Thibeault, and R. Hoffmann, *J. Am. Chem. Soc.* **100,** 3686 (1978).
20. R. Ramírez and M. C. Böhm, *Int. J. Quantum Chem.* **30,** 391 (1986).
21. R. Ramírez and M. C. Böhm, *Int. J. Quantum Chem.* **34,** 571 (1988).
22. R. Hoffmann, *Angew. Chem. Int. Ed. Engl.* **26,** 846 (1987).